An Analysis of Nondifferentiable Models of ΣΔ and DPCM Systems From the Perspective of Noninvertible Map Theory

INA TARALOVA-ROUX AND ORLA FEELY
Department of Electronic and Electrical Engineering
University College Dublin
Belfield, Dublin 4
IRELAND

Abstract: - Two electronic engineering systems modelled by nondifferentiable noninvertible maps, the Differential Pulse Code Modulation (DPCM) system and bandpass ΣΔ modulator are investigated. Although quantitative similarities can be observed through the comparative analysis of phase and parameter planes, these two systems present different features when analysed from the perspectives of the theory of noninvertible maps and that of nonlinear dynamics. It is shown that the models obtained correspond to noninvertible maps of different kind; and also that periodic solutions of opposite stability can be observed only in the case of DPCM, moreover, the basins of attraction are bordered by different type of singularities: critical lines and their preimages of different order for the Sigma-Delta Modulator, and stable manifolds of saddle points on the basin frontier for the DPCM. The dynamics of the two systems are shown to become more similar when the parameters approach the centre bifurcation, which is shown to be particular to the nondifferentiable models. At the centre bifurcation the observed behaviour is more complex for the Sigma-Delta Modulator.

Key-Words: - Noninvertible Maps, Nonlinear Dynamics, Bifurcations, Critical Lines, DPCM, Sigma-Delta Modulator

IMACS/IEEE CSCC'99 Proceedings, Pages:3081-3086

1 Introduction

Both Differential Pulse Code Modulation (DPCM) systems and Sigma-Delta (ΣΔ) Modulators are engineering systems widely used in practice. DPCM systems are based on prediction and quantization. They are used in transmission for bit rate reduction, for example in digital phone networks [3]. Bandpass sigma-delta (ΣΔ) modulators [1,2] are used in data conversion systems in areas such as RF communication systems and spectrum analysers. The purpose of this work is to compare these two systems from the perspective of noninvertible map theory, the starting point for comparison being that both systems are modelled by nondifferentiable models.

A first investigation has already been carried out to compare these two systems in the vicinity of the foci destabilisation bifurcation, known in the differentiable case as the Neimark-Hopf bifurcation [5]. The results obtained showed qualitative similarity of the corresponding phase planes of both systems at the bifurcation point. Nevertheless, our current studies show that the destabilisation of the foci in the case of nondifferentiable models takes place in a qualitatively different way when compared to the Neimark-Hopf bifurcation, and for this reason we refer to it as a "centre" bifurcation. Moreover, when analysing the two models as noninvertible maps and for broader parameter values, *qualitative* differences between the two systems can be observed. In order to better understand these differences, Section 2 is devoted to a short review of noninvertible maps. Section 3 describes the system models, and section 4 discusses differences and similarities between the two models. A concluding section ends the paper.

2 Review of Noninvertible Maps

If we consider the dynamics of a system described by any map in the state space, we refer to the notion of a *noninvertible* map when the state space contains regions where the backward iterate (also called *preimage*) of a point under the map is not unique, or does not exist. This also means that a point of the state space may result from the iteration of distinct starting conditions. Then the regions Zi of the state space with different number i of preimages are separated by segments of critical curves, called LC from *ligne critique* in French [4]. One can thus consider the regions with more than one preimage as a superposition of *i* sheets, where each sheet corresponds to a given *rank-one* preimage (*first* backward iterate). Therefore, when the LC are crossed, the number of first rank preimages changes.

Another important notion to which we shall refer hereafter is the notion of singularities in the particular context of two dimensional map *T*. A *k*-cycle (order k cycle or period k cycle) of *T* consists of k iterated points (images) satisfying $X = T^k X$ with $X \neq T^l X$, for $1 \leq l < k$, l and k being integers. A fixed point is a cycle with $k = 1$. The nature of fixed points and order *k* cycles can be determined using the eigenvalues of the Jacobian matrix. Let S_j, j=1,2 be the two eigenvalues,

a) $|S_1| > 1$ and $|S_2| < 1$, X^* or (X_i), i=1,...,k is a saddle,

b) $|S_1| > 1$ and $|S_2| > 1$, X^* or (X_i), i=1,...,k is an unstable node,

c) $|S_1| < 1$ and $|S_2| < 1$, X^* or (X_i), i=1,...,k is a stable node.

Similarly, when the eigenvalues are complex, i.e. $S_1 = \rho e^{-j\varsigma}$, $S_2 = \rho e^{+j\varsigma}$

d) $\rho < 1$, X^* or (X_i), i=1,...,k is a stable focus.

e) $\rho > 1$, X^* or (X_i), i=1,...,k is an unstable focus.

When the eigenvalues are on the unit circle, the system is on the limit of stability.

Other kind of singularities are the stable and unstable manifolds associated with fixed and periodic points.

If P* is an unstable fixed or periodic point, and U is a neighborhood of P*, the *local* (i.e. in U) unstable manifold of P* is defined as the set of the points of U whose consecutive preimages converge towards P*. The *global* unstable manifold is the set of points which consecutive preimages exist and converge towards P*. It can be constructed by plotting the images of the local unstable manifold. The same reasoning can be applied to the stable manifold. The global stable manifold can be constructed by plotting the preimages of the local stable manifold.

To study the behaviour in the system under consideration, we require also knowledge about the regions of existence of the periodic points, the more complex chaotic attractors, and their *basins* of attraction (i.e. the range of initial conditions from which trajectories converge towards an attractive solution - periodic point or chaotic attractor).

By *bifurcation* we understand a qualitative change in the system behaviour (local or global) under some particular parameter variations. When the parameter vector dimension is greater than one, bifurcations occur over a curve (surface in 3D) called a *bifurcation curve*. Bifurcation curves are summarized in *bifurcation diagrams* and enable a priori knowledge of the system convergence or divergence, chaotic or periodic behaviour.

3 System Models

DPCM (see Fig.1) is a data compression technique based on error transmission. The differential part of the DPCM system is used to reduce the signal flow before its A/D conversion and is based on the following coding principle: as the successive signal values are usually correlated, it would be desirable to make use of this transmission redundancy, without in any way losing information. Therefore, rather than transmitting the signal itself, only the prediction error e, i.e. the difference between the predicted $\hat{s}$ and the effective s signal value, is quantized and transmitted. The difference between the two correlated signals is thus coded in a smaller number of bits, and so the transmission data flow is reduced. The input-output system is shown in Fig.1. The input signal s has to be reconstructed at the end of the chain. The reconstructed signal is called s'. At the encoder, the predicted value $\hat{s}$ of the input signal s is calculated based on its past samples by the recursive linear filter R. The encoder of the system (Fig.1) includes a nonlinear element - the quantizer. The latter is approximated by a piecewise linear characteristic containing points of non-differentiability. Structurally similar is the scheme of the bandpass $\Sigma\Delta$ system (Fig.2) whose quantizer is represented by a sign function. $\Sigma\Delta$ systems operate in discrete time and convert an analogue input signal x into a low-resolution high-speed stream of bits. In the case of a bandpass $\Sigma\Delta$ system, the goal is to shape the quantization noise away from the narrow band in which the input signals will lie, so that it can subsequently be removed.

An ideal second-order bandpass $\Sigma\Delta$ modulator has noise transfer function zeroes at $e^{\pm j\theta}$, where θ is chosen to centre the passband at any required frequency $f_0 = f_s.\theta/2\pi$ (f_s is the sampling frequency). In a practical implementation of this system, finite op amp gain will alter the noise transfer function zeros from $e^{\pm j\theta}$ to $re^{\pm j\theta}$, where $r < 1$.

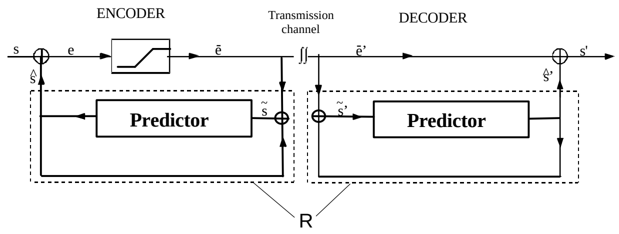

Fig.1 DPCM Transmission system

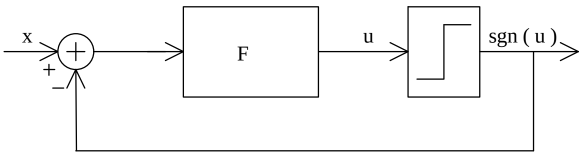

Fig.2 Bandpass ΣΔ modulator

With noise transfer function zeros at $re^{\pm j\theta}$ and zero input, the system of Fig.2 is modelled by the equation

$$u_n = 2r\cos\theta(u_{n-1} - \operatorname{sgn} u_{n-1}) - \\ - r^2(u_{n-2} - \operatorname{sgn} u_{n-2}) \qquad (1)$$

By choosing the new variables $x_n = u_{n-1}$ and $y_n = u_n$ and the state vector $X_n = (x_n\ y_n)^t$, the resulting map T in $R^2 \to R^2$ is obtained for the ΣΔ system : $X_{n+1} = T(X_n)$

$$T:\begin{cases} x_{n+1} = f(x_n, y_n) = y_n \\ y_{n+1} = g(x_n, y_n) = -r^2(x_n - \operatorname{sgn} x_n) + \\ +2r\cos\theta(y_n - \operatorname{sgn} y_n) \end{cases} \qquad (2)$$

A corresponding substitution can be applied to the DPCM system, by selecting the new variables: $x = \hat{s}(k-1)$ and $y = \hat{s}(k)$

$$T := \begin{cases} x_{n+1} = f(x_n, y_n) = y_n \\ y_{n+1} = g(x_n, y_n) = a_2[x_n + q(x_n)] + a_1[y_n + q(y_n)] \end{cases} \qquad (3)$$

$$\text{with } q(z) = \begin{cases} p(s-z) & if\ |s-z| < \dfrac{1}{p} \\ sign(s-z) & if\ |s-z| > \dfrac{1}{p} \end{cases} \qquad (4)$$

p is the DPCM quantizer slope and is called the companding gain, it is chosen larger than one in order to amplify the signal-to-noise ratio when the quantizer input is small. For both systems, T belongs to the class of piecewise-continuous noninvertible maps.

4 Results and Discussion

4.1 Comparison of the ΣΔ and DPCM maps

If we compare the two maps (2) and (3), it may be seen that because of the different nonlinearity of the quantizer, the ΣΔ map is of the type Z1/Z2/Z1 while the DPCM map is of the type Z1/Z3/Z1. For both systems, the Zi (i>1) region is enclosed between the two critical lines segments LCa and LCb (the region Zi consists of points with i preimages), see Figs.3, 4. The case when the number of preimages changes by one when crossing the critical lines is typical only for piecewise continuous maps, while the case when the number of preimages changes by two when crossing the critical lines is typical for all other maps and is therefore much more studied in theory. By that criterion the DPCM map is closer to continuous maps.

4.2 Centre bifurcation

For $\rho<1$ (ΣΔ) and $a_2<-1$ (DPCM), we observe the existence of stable foci for both systems, more of which appear as ρ gets closer to 1, and a_2 to –1. An important bifurcation particular and common to both ΣΔ and DPCM systems, not encountered in the differentiable case, is related to the destabilisation of the foci. In the differentiable case, the Neimark-Hopf bifurcation characterises the destabilisation of the focus and the emergence of an invariant closed curve in the vicinity of the destabilised focus. In the case of our two systems, described by piecewise linear functions, at the bifurcation value the fixed (periodic) focus point becomes a centre, as locally the map is linear, but not globally.

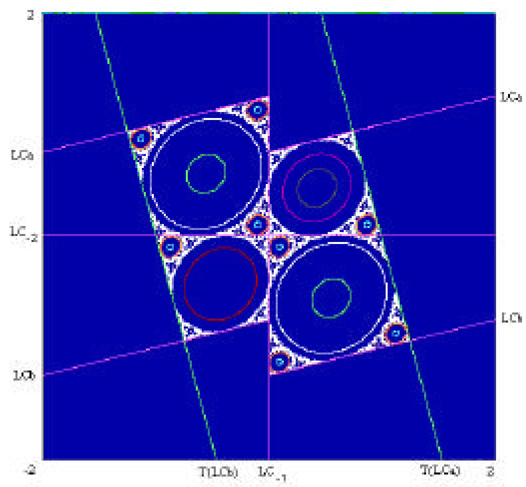

Fig. 3 Centre bifurcation ΣΔ $\cos\theta$=0.125 r=1.00

Thus at the bifurcation value trajectories trace out elliptical orbits, lying on closed invariant curves around the fixed and periodic points, together with more complex trajectories as shown in Figs.3, 4.

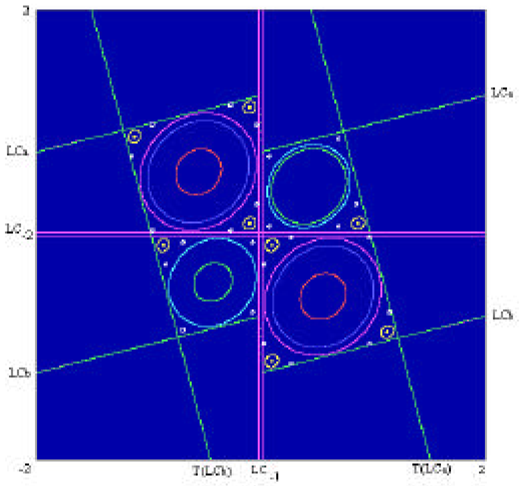

Fig. 4 Centre bifurcation DPCM a_1=0.25 a_2=-1.00

This behaviour lies within an invariant region, bounded by the critical lines and their first rank images. But the main difference with respect to the differentiable case can be seen after the bifurcation value, when the fixed point becomes a repelling focus. Now the trajectories spiralling out from the focus do not diverge to infinity, but the nonlinear effects give rise to the appearance of some closed invariant set which is generally far from the fixed point (Figs. 5,6). How far depends on the location of the critical lines.

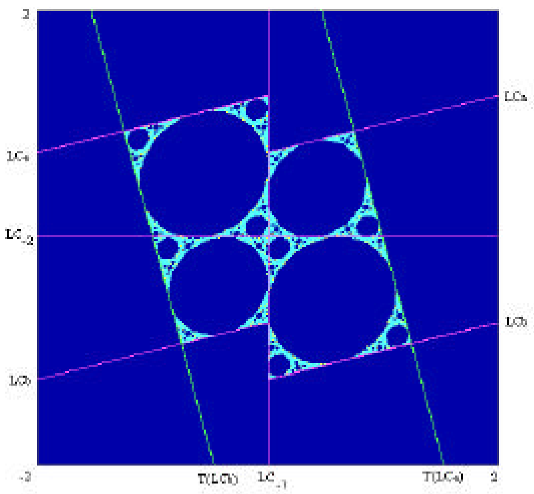

Fig. 5 After the centre bifurcation,
$\Sigma\Delta$ $\cos\epsilon$=0.125 r =1.001

Moreover, at the bifurcation, centres of different period can coexist (multistability). This phenomenon is illustrated in Figs. 3-4. Because of the difference with the Neimark-Hopf bifurcation we refer to that bifurcation as a centre bifurcation.

Again comparing the two systems one can notice that an additional, more complex trajectory (in white) is observed in the case of the $\Sigma\Delta$ modulator (Fig.3), while all trajectories remain of only centre type for the DPCM.

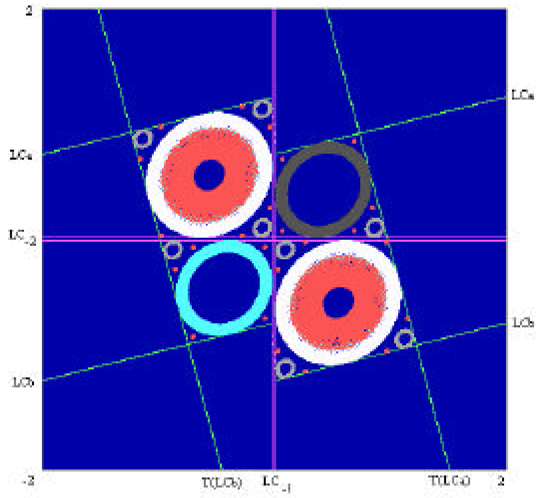

Fig. 6 After the centre bifurcation,
DPCM a_1=0.25 a_2=-1.001

4.3 Basin frontier

In our previous study [5] we have analysed the importance of the critical lines as limiting the absorbing areas within which all system trajectories are captured. In this section, we are concerned with another important issue of nonlinear dynamics, namely finding what singularities form the limits of the basins of attractions for the two systems.

Indeed, by using the methods and tools of noninvertible maps, we are able to explain also the dynamics within the basin of attraction. In fact, we shall see that the evolution of the phase trajectories is strictly determined by the invariant manifolds of the nonattractive singular points (DPCM) or by the preimages of the critical curves ($\Sigma\Delta$). These singularities of higher order allow us also to analyse the type of frontiers (fuzzy, connected, non-connected) which exist between the different basins.

Let consider first the DPCM case where we shall see that some periodic points of saddle type located on the frontier of the basin allow us to determine this frontier. In order to calculate the stable and unstable manifolds of the periodic points associated with the DPCM system, we assume that the saddle points do not lie on the lines of discontinuity of the map T i.e. the map T is assumed to be differentiable at the vicinity of the points of the saddle cycle.

Let consider now as an example the case when the basins of a stable period 11 node and a stable period 11 focus coexist (Fig.7).

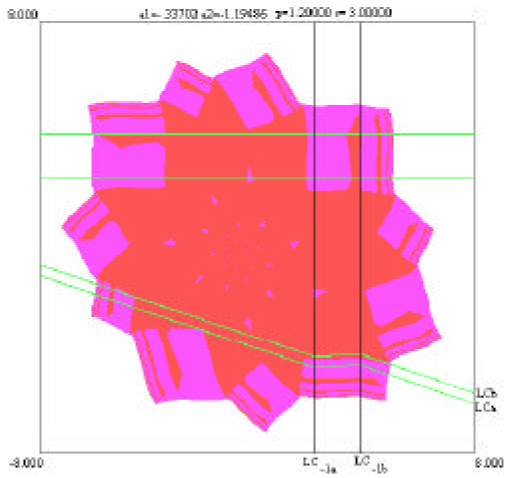

Fig.7 DPCM, basins of attraction of the stable node 11 and focus 11

An analysis shows that 4 saddle points of period 11 are located on the frontier of the two basins. Let call the first points of each period 11 saddle C1, C2, C3 and C4 respectively. To find the frontier, let us trace the corresponding stable and unstable manifolds to the four period 11 saddles. As initialisation, we start with the coordinates of the saddle points located on the frontier of the basin.

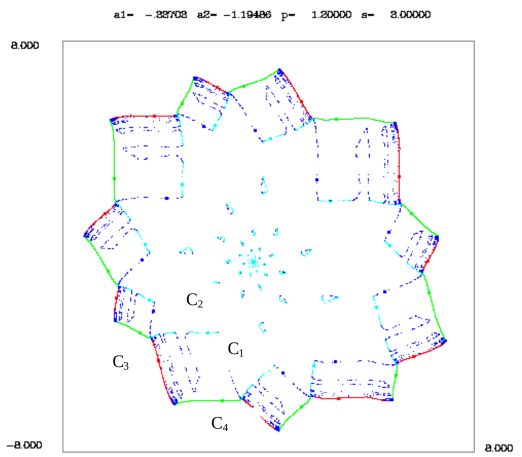

Fig.8 DPCM, borders of the basins of attraction given by the stable manifolds of the four saddles of period 11 $C_1C_2C_3C_4$

Then, we proceed to a linear approximation of the stable manifolds in the vicinity of the points of these saddles (the unstables manifolds converge towards the points of the attractive period 11 node and focus). It can be seen that the stable manifolds associated with the saddles C_1, C_2 form the frontier of the basin of the node 11 and are represented in pale grey (Fig.8). The stable manifolds associated with the saddles C_3, C_4 form the frontier of the basin of the focus 11 and are coloured in dark grey (Fig.8). The set of preimages of the stable manifolds associated to the saddles C_3 and C_4 form the islands in the basin of the focus 11.

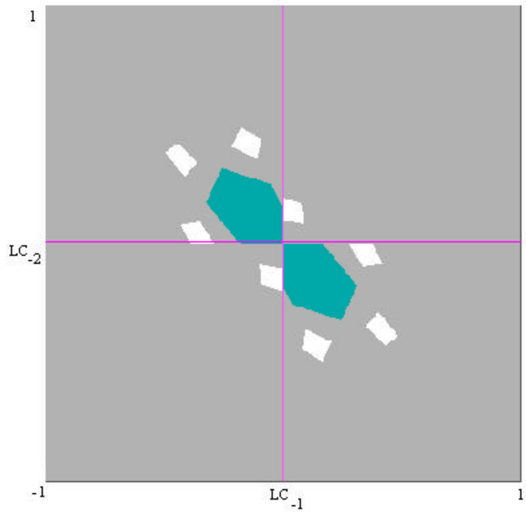

Fig.9 ΣΔ, basins of attraction of the stable foci

In the case of the ΣΔ system, at all points where the map T is differentiable, its Jacobian matrix is

$$\begin{pmatrix} 0 & 1 \\ -r^2 & 2r\cos\theta \end{pmatrix} \qquad (5)$$

which has eigenvalues at $re^{\pm j\theta}$. Thus when $r < 1$ all fixed and periodic points of T are stable foci, and there are no unstable periodic points. In this case, the boundary of the basin is made of segments of the set LC_{-1} and its increasing rank preimages LC_{-k}.

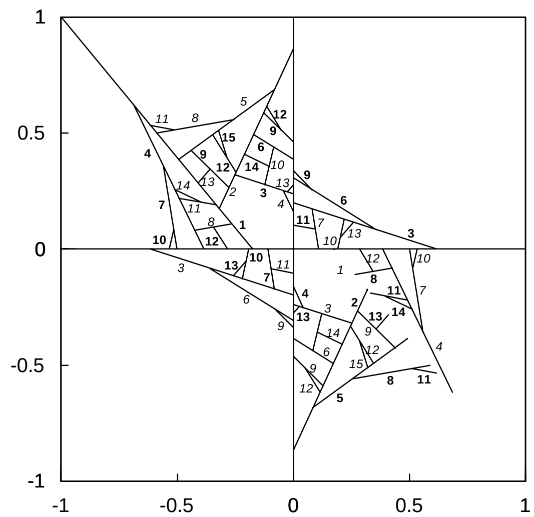

Fig.10 ΣΔ, borders of the basins of attraction given by the preimages of the critical lines LC_{-k}

It is intuitively clear why this should be the case –

the only reason for two nearby points to converge to different locations is that after some number of iterations their iterates land in different quadrants, i.e. the two initial points must lie on opposite sides of some preimage of one of the axes. As an example, Fig. 9 shows the basins of attraction for r= 0.97 and $\cos\theta=-0.4$ and Fig. 10 labels the preimages of Fig.9 with the preimages of positive x axis shown in bold and numbered in bold according to their order, and the preimages of the negative x axis numbered in italics.

5 Conclusion

Two electronic systems, the ΣΔ Bandpass Modulator and the DPCM both modelled by nondifferentiable noninvertible maps have been analysed and compared from the perspective of the nonlinear dynamics. It has been shown that the two systems give rise to a different kind of map, Z1/Z2/Z1 for the ΣΔ and Z1/Z3/Z1 for the DPCM. But despite the different map describing each of the systems, similar features for both nondifferentiable models have been observed and explained, such as the centre bifurcation, which does not exist in the case of differentiable models. This difference arises from the piecewise linearity of the maps, and is characterised among others by the fact that there is not an invariant closed curve after the bifurcation.

The two systems have also been shown to differ by the nature of the critical set which limits the frontier of the basins of attraction: stable invariant manifold of the nonattractive singular points for DPCM, and the set of preimages of critical curves for ΣΔ.

Finally, we hope that this analysis has contributed to the better understanding of the dynamical behaviour of these two electronic systems and also to the development of the noninvertible map theory for the case of nondifferentiable models.

References:

[1] Feely O., Fitzgerald D., Nonlinear Dynamics of Bandpass Sigma-Delta Modulation, *Proc. IEEE Int. Symp. On Circuits and Systems, Atlanta, GA*, IEEE, New York, 1996, p. III: pp.146 – 149.

[2] R.Schreier and M. Snelgrove, Bandpass sigma-delta modulation, *Electron. Letters* 25, 1989, pp.1560-1561.

[3] Macchi O., Uhl C., Stability of the DPCM transmission system, *IEEE Trans. CAS*, Vol.39, No.10, 1992, pp.702-722.

[4] Mira C., Gardini L., Barugola A., Cathala J.C., *Chaotic Dynamics in Two Dimensional Noninvertible Maps*, World Scientific, Series A, vol. 20, 1996.

[5] Taralova-Roux I. and O.Feely, A Comparative Study of DPCM Encoder and Bandpass Sigma-Delta Modulator in the Vicinity of the Hopf Bifurcation, *Proc. of the International Symposium on Non-linear Theory and its Applications NOLTA'98*, 14-18 September 1998, Crans-Montana, Switzerland Vol.2 pp. 755-758